Numerical simulations of piano strings. II. Comparisons with measurements and systematic exploration of some hammer-string parameters

Antoine Chaigne
Signal Department, Telecom Paris, CNRS URA 820, 46 rue Barrault, 75634 Paris Cedex 13, France

Anders Askenfelt
Department of Speech Communication and Music Acoustics, Royal Institute of Technology (KTH), P. O. Box 700 14, S-100 44 Stockholm, Sweden

(Received 26 May 1993; accepted for publication 30 November 1993)

A physical model of the piano string, using finite difference methods, has recently been developed. [Chaigne and Askenfelt, J. Acoust. Soc. Am. **95**, 1112–1118 (1994)]. The model is based on the fundamental equations of a damped, stiff string interacting with a nonlinear hammer, from which a numerical finite difference scheme is derived. In the present study, the performance of the model is evaluated by systematic comparisons between measured and simulated piano tones. After a verification of the accuracy of the method, the model is used as a tool for systematically exploring the influence of string stiffness, relative striking position, and hammer-string mass ratio on string waveforms and spectra.

PACS numbers: 43.75.Mn, 43.75.Wx

INTRODUCTION

In a previous paper, a physical model of the piano string with particular emphasis on a time-domain modeling close to the basic equations has been presented.[1] The model, which is based on the one-dimensional equations of a damped, stiff string interacting with a nonlinear hammer, is put into a numerical form by the use of standard finite difference methods. The compression characteristic of the hammer, being one of the most essential components, is modeled by a power law. Using this model, principal quantities like string displacement and velocity, the interacting force between hammer and string, and the force exerted by the string on the bridge, can conveniently be computed for different combinations of hammer and string parameters.

The model has now been evaluated for a large number of cases by comparing simulated waveforms with measurements on real pianos. The comparisons included a set of representative notes of the piano from the bass, mid, and treble register, played at different dynamic levels, and with different hammers. The hammer-string parameters used in the simulations were obtained from measurements.

After the method had been verified to reproduce measured waveforms satisfactorily, the model was used for a systematic exploration of some of the hammer-string parameters and their influence on string waveforms and spectra. The underlying theory of the struck string and the principal dependence of the hammer-string parameters is now well known,[2,3] but in many cases an experimental verification has been lacking due to the practical difficulties of reaching a desired step-by-step variation in only one parameter at a time. For this purpose, a numerical simulation is particularly well suited, and several investigators have tried this approach, using models of varying degree of refinement.[1] This study adds a more systematic approach, using a model which has been verified to generate realistic results. The parameters included in the present part II of the study are relative striking position, hammer-string mass ratio, and string stiffness, which all attract a particular interest since their exact values appear to be crucial for piano design.

I. COMPARISON BETWEEN REAL AND SIMULATED PIANO STRING VIBRATIONS

In this section, the numerical model is evaluated by comparing simulated string and hammer waveforms with previously measured signals in real pianos.[4,5] Other examples of comparisons between real and simulated waveforms can be found in previous works on piano strings based on different numerical techniques.[6,7]

The numerical values of all physical parameters used in the present experiments are given in Table I. Some of the parameters were measured by the authors, while others were extracted from the literature.[3,5,8] The parameters of the hammer felt (stiffness coefficient K, nonlinearity exponent p), and the damping coefficients of the string (b_1, b_3)[1] were estimated from experimental data by means of standard curve-fitting procedures.

A. Bass, mid, and treble

A first check of the model was made by computing the string waveforms for a few notes in different ranges of the piano. In order to clearly illustrate the propagation on both sides of the hammer, it was decided to observe the velocities at some distance from the striking position rather than at that point. Figure 1 shows a comparison between the simulated and observed string velocities at 40 mm from the striking point towards the bridge, for a treble (C7), midrange (C4), and bass note (C2), respectively. It can be

 0001-4966/94/95(3)/1631/10/$6.00

TABLE I. Values of the parameters used in the simulations.

Parameters		C2	C4	C7	Units
String					
fundamental frequency	f_1	65.4	262	2093	Hz
string length	L	1.90	0.62	0.09	m
total string mass	M_S	35.0(×2)	3.93(×3)	0.467(×3)	g
string tension	T	750	670	750	N
Young's modulus	E	2.0×10^{11}	2.0×10^{11}	2.0×10^{11}	N/m^2
string stiffness parameter	ϵ	7.5×10^{-6}	3.82×10^{-5}	8.67×10^{-4}	
damping coefficient	b_1	0.5	0.5	0.5	s^{-1}
damping coefficient	b_3	6.25×10^{-9}	6.25×10^{-9}	2.6×10^{-10}	s
Hammer					
relative striking position	α	0.12	0.12	0.0625	
hammer mass	M_H	4.9 (×2)	2.97 (×3)	2.2 (×3)	g
stiffness nonlinear exponent	p	2.3	2.5	3.0	
coefficient of hammer stiffness	K	4.0×10^{8}	4.5×10^{9}	1.0×10^{12}	
hammer-string mass ratio	M_H/M_S	0.14	0.75	4.71	
Sampling					
sampling frequency	f_e	16	32	96	kHz
number of string segments	N	100	50	16	

seen that the model is able to reproduce the waveforms quite well over the whole register of the piano, including the details of the attack transients. Small discrepancies which can be observed in the actual timing relations between the pulses are mostly due to slight differences in observation points. In the C2-example, the agraffe reflection during string contact (the first negative pulse) is not reproduced accurately. This discrepancy is likely due to either a nonrigid string termination at the agraffe in the real piano, or an interference with reflections from the end of the string wrapping. These two phenomena are not taken into account in the model.

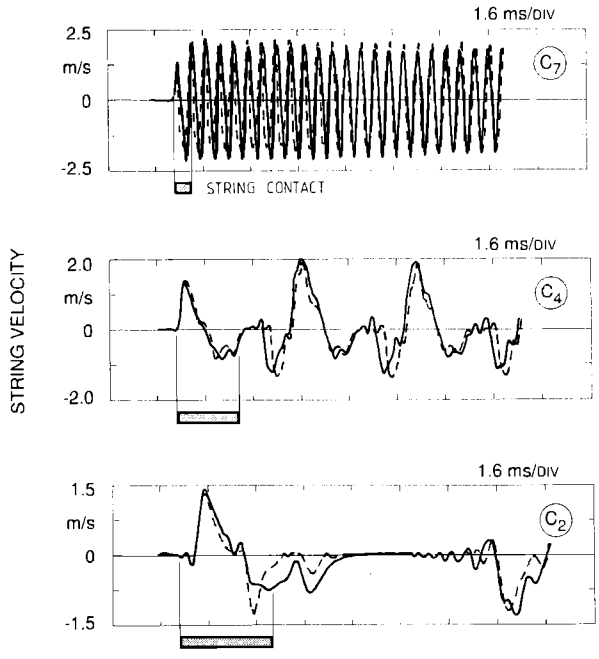

FIG. 1. String velocity at the bridge side of the striking point (40 mm from the hammer) for a bass, mid, and treble note (C2–C4–C7), played *mezzo forte;* measured[4] (full line) and simulated (dashed). The measured hammer-string contact duration is included for reference.

The computed forces between hammer and string for the C7, C4, and C2 examples above are shown in Fig. 2. This variable is of particular interest as it determines the string spectra.[9] The actual history of the hammer force is difficult to measure under normal conditions,[10] and an indirect estimation by a measurement of the acceleration at the wooden hammer moulding is normally the closest alternative. Such measurements, which have been extensively investigated in a previous work by the second author, are not reported in the present paper.[11]

The simulations emphasize the strong effect of the reflections from the agraffe during hammer string contact, clearly seen in the C4 and C2 examples. Each reflection results in a temporary increase in interacting force, corresponding to a downward impulse on the hammer. As dis-

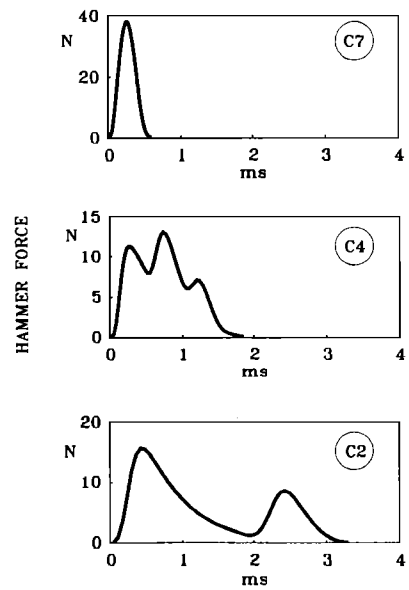

FIG. 2. Simulated hammer forces corresponding to Fig. 1. Initial hammer velocity $V_{H0}=2.5$ m/s.

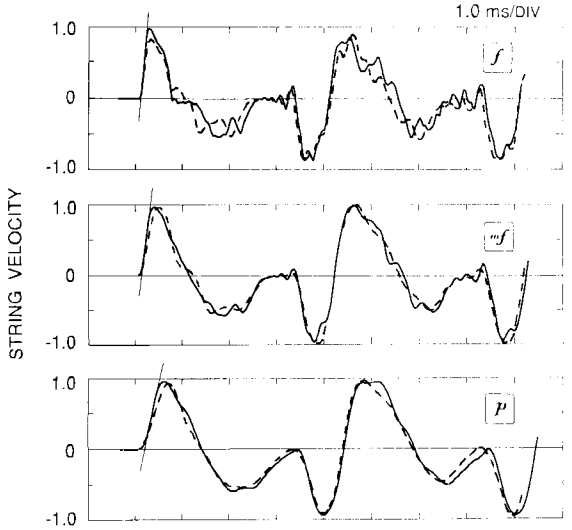

FIG. 3. Comparison of string velocities at three dynamic levels, *forte-mezzo forte-piano.* (C4, observation point at the bridge side, 40 mm from the hammer). Measured waveform (full line),[5] and simulated (dashed) with initial hammer velocity (V_{H0}) equal to 4.0, 1.5, and 0.5 m/s.

cussed by Hall, these reflections are one of the major mechanisms of hammer release.[12]

The peak force in these examples at *mezzo forte* level were about 40, 13, and 16 N, for strings C7, C4, and C2, respectively. The high value for the C7 example is due to the pronounced nonlinearity of the treble hammers (in this case $p=3.0$). The hammer-string contact durations obtained in the simulations were 0.6 ms (C7), 1.9 ms (C4) and 3.25 ms (C2), respectively, which is in close agreement (within 6%) with the experimentally observed values (0.6; 2.0; 3.1 ms).

B. Dynamic level

One of the most important control parameters for the piano player is the initial hammer velocity (V_{H0}). By varying this parameter in our nonlinear physical model, both the level and frequency content of the simulated tones will change, like in real pianos. This ability of the model is illustrated in Fig. 3 which shows a comparison of measured and simulated waveforms of the string velocity for note C4 played at three different levels: *forte, mezzo forte,* and *piano.* The plots are presented on a normalized amplitude scale. Like in Fig. 1, the velocities were observed at 40 mm from the hammer on the bridge side. In the synthesis, the initial hammer velocities were 4.0, 1.5, and 0.5 m/s, respectively.

Again, the simulations reproduce the main features of the measured waveforms convincingly, including the steepening of the initial slope and general shortening of the pulses with increasing dynamic level. Also, the contribution from string stiffness, clearly visible in the *forte* example as a "ripple" with increasing amplitude at the end of the first period, is nicely reproduced in the simulations (see also Sec. II A). The major difference between measurements and simulations is found at the first agraffe reflections in the *forte* example where a complete match was not

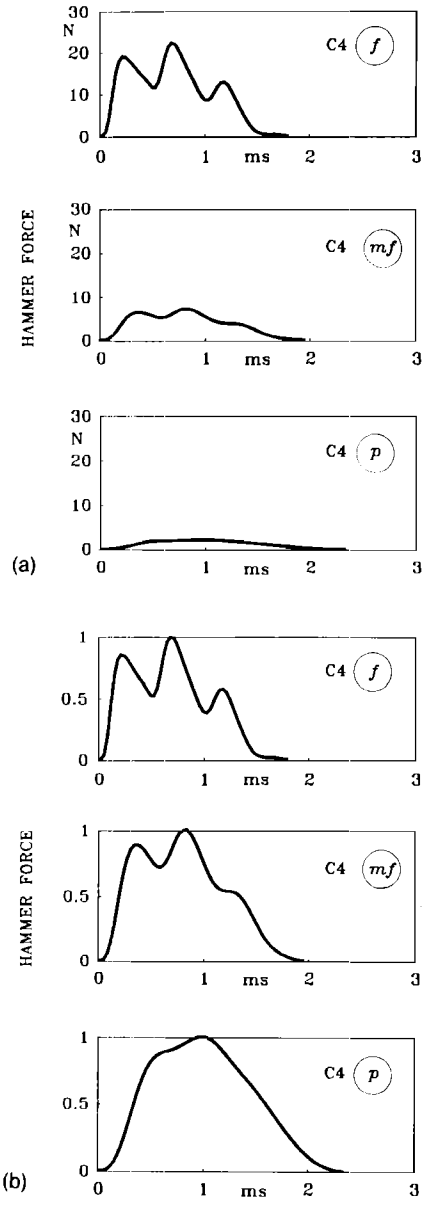

FIG. 4. Simulated hammer forces for note C4 at three dynamic levels *(f-mf-p)* corresponding to Fig. 3; (a) absolute values in N; (b) normalized.

reached, possibly indicating a slight discrepancy in the hammer parameters between the real and simulated case.

The calculated hammer forces corresponding to the three examples at *forte, mezzo forte,* and *piano* levels in Fig. 3 are shown in Fig. 4(a). The simulations show, in particular, how the nonlinear stiffness narrows the force pulses as the initial hammer velocity is increased. The peak force increases from about 2 N at *piano* to 22 N at *forte.* The normalized plots in Fig. 4(b) illustrate clearly how the waveform of the hammer-string force sharpens as the dynamic level is increased. Also the effect of the agraffe reflections becomes more prominent.

As expected, the spectra of the string velocity for the three cases show an increasing spectral content with increasing hammer velocity (see Fig. 5). A comparison between the measured and simulated spectra reveals that there are rather large differences above the first 5–7 par-

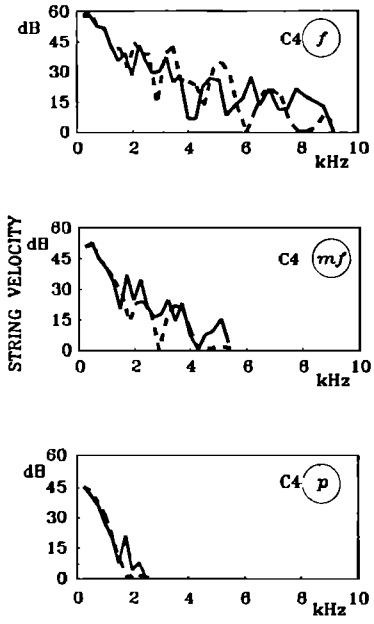

FIG. 5. Spectral envelopes corresponding to the initial 32 ms of the simulated string velocities at three dynamic levels (*f-mf-p*) in Fig. 3 (dashed lines). The measured spectral envelopes are included for comparison (full lines).[4]

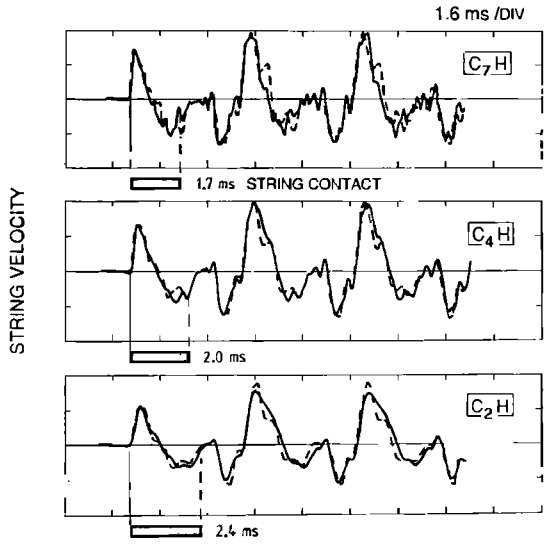

FIG. 6. Comparison of string velocities for note C4 played with a treble (C7H), original (C4H) and a bass hammer (C2H); as measured (full lines),[4] and simulated (dashed). Approximate scale units are 1 m/s. The measured hammer-string contact durations are included for reference.

tials, in spite of the seemingly close match in waveform in Fig. 3. In particular, the *forte* example shows local discrepancies of the order of 10–15 dB, which for the higher modes, however, can be partially attributed to the limited spatial resolution of the numerical modeling. Noticing that the maximum deviation between exact and approximate location of the striking point is equal to half the spatial step, then the spatial resolution can be written $L/2N$ (see Table I for the definition of variables and symbols). As a consequence, the partials' frequencies will not be correct, and this error will in turn influence the spectral envelope. An estimate for the frequency shift of the nth-partial consecutive to a difference between real and modeled hammer location can be found by writing that the product of the wave number by the distance of hammer from agraffe is constant, which is equivalent to

$$\Delta f_n = f_n \frac{1}{1+2N\alpha}, \tag{1}$$

where α is the relative hammer striking position.

With the parameters listed in Table I for note C4, Eq. (1) predicts, for example, a frequency shift of nearly 400 Hz for partials near 5 kHz, which is in close agreement with the spectra presented in Fig. 5. Other discrepancies still remain, especially for the highest partials in the *forte* case, which cannot be explained with our model.

C. Hammer properties

A key parameter in piano design is the compression characteristic of the hammer. For this reason, it was interesting to verify that the numerical model reproduces the main features of a measured waveform, using reasonable estimates of hammer parameters K and p.[1] In the previous experiments on real pianos, the hammer parameters were changed both in a straightforward manner by exchanging hammers, and also in the traditional way by voicing.[5,8]

A comparison of real and synthesized waveforms for the note C4 played with exchanged hammers (C7, C4, and C2 hammer) is given in Fig. 6. The main differences between the three hammers are found in the stiffness (p and K), increasing from bass to treble, but also the mass differs (see Table I). Again, a convincing match in waveform is seen, possibly with a somewhat more peaked appearance of the simulated waveforms. The corresponding spectra in Fig. 7 show a similar amount of high-frequency content for the measured and simulated cases, respectively. Like in Fig. 5, a frequency shift in the modeled spectral envelope can be observed, relative to the measured, whose order of magnitude is given by Eq. (1). In line with expectations, the spectra grow richer with increasing hammer stiffness.

The hammer forces for the three hammer-string combinations are shown in Fig. 8, where it can be seen how the smoothness of the force pulses is changed by shifting hammers. With the soft, and more massive bass hammer, the agraffe reflections are almost filtered out. Also the contact duration changes slightly, increasing with the softer and heavier bass hammer, and decreasing with the harder and lighter treble hammer. However, these changes are relatively small, about 0.1 ms (±5%). The changes are smaller than those observed experimentally (about ±15%), possibly indicating a small error in the estimation of the hammer parameters.

In summary, the experiments show that the model gives realistic simulations of the piano string for notes in different pitch ranges, at different dynamic levels, and played with different hammers. These results are in agreement with those obtained by other authors using different modeling techniques.[3] Most of the discrepancies which occur can be explained by slight mismatches in string-

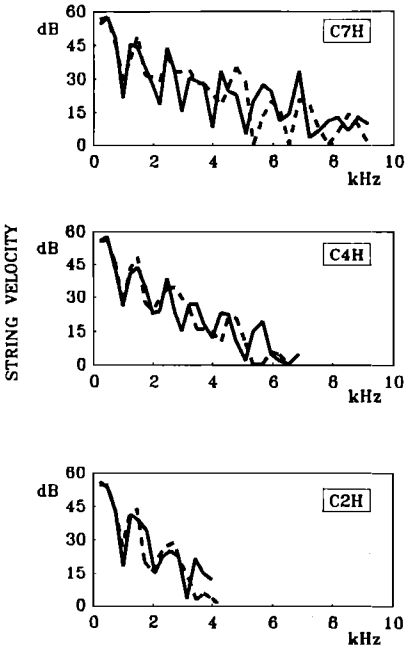

FIG. 7. Spectral envelopes corresponding to the initial 32 ms of the simulated string velocities in Fig. 6 with three different hammers (C7H-C4H-C2H) striking note C4 (dashed). The measured spectral envelopes are included for comparison (full lines).[4]

hammer parameters, and by the limited spatial resolution. The comparison between spectra of real and simulated tones show, however, additional differences which cannot be simply explained with the help of our model, especially for frequencies above 3 kHz. At present, it cannot be concluded whether they are due to small errors in the measurements, or to insufficient modeling of the system. Since these discrepancies primarily refer to spectral components whose magnitude are at least 30 dB below the fundamental, we could still be rather confident in using the model for predictions.

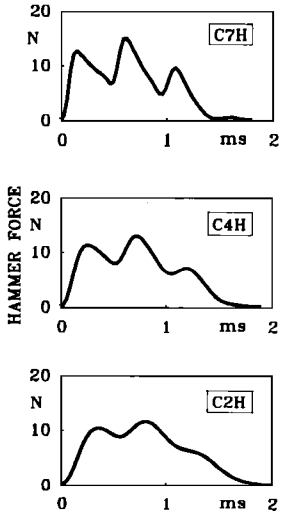

FIG. 8. Simulated hammer forces corresponding to Fig. 6 with three different hammers (C7H-C4H-C2H) striking note C4.

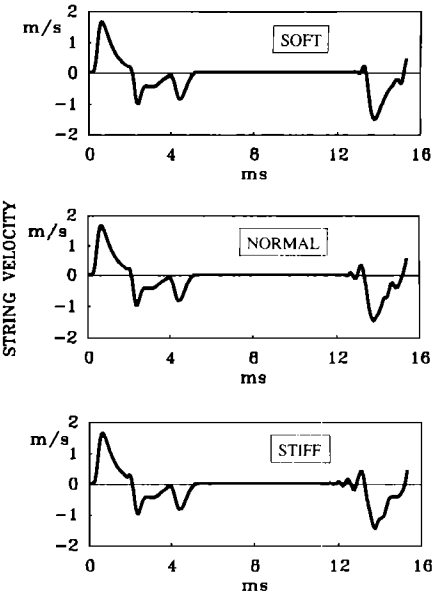

FIG. 9. Influence of string stiffness. Simulated string velocities of a bass note (C2) for three cases with increasing stiffness; soft (-50%), nominal, and stiff ($+50\%$). The value of the stiffness parameter was $\epsilon = 5.0\times10^{-6}$, 7.5×10^{-6}, and 11.25×10^{-6}, respectively.

II. SYSTEMATIC VARIATIONS OF HAMMER AND STRING PARAMETERS

In the previous section, the goal was to assess the power of our numerical model in reproducing the main features of real piano strings. It was shown, in particular, how the model was able to account successfully for the influence of both initial hammer velocity and felt compression properties. These simulations confirm the basic assumptions on the behavior of piano strings developed in the past few years by several authors.[2,3]

In this section, our model is used as a tool for systematically exploring the influence of some hammer and string parameters on string waveforms and spectra. The parameters selected for the numerical experiments included string stiffness, hammer-string mass ratio, and relative hammer striking position ("striking ratio"). These parameters are relatively difficult to change experimentally, so a numerical method lends itself particularly well for this purpose, once the method has been verified to perform satisfactorily. The general approach used here was to start from the measured values of the parameters (given in Table I), and proceed by varying one parameter at a time, step by step.

A. String stiffness

In Fig. 9, the string velocity waveform of a bass note (C2) is shown as the string stiffness is varied by $\pm50\%$ compared to its nominal value (see Table I). It is seen that the major effect of increasing the stiffness is to enhance the transverse precursor preceding the reflection from the bridge. The example is a nice illustration of the ability of our numerical model to reproduce dispersive effects due to stiffness directly in the time domain. The interesting question of the perceptual importance of the transverse precur-

sor has not been studied as yet, but it might be smaller than expected. In particular, at the very beginning of the note, where one could expect a weak, but early, component to be audible, the transversal string precursor is masked by longitudinal string motion.[13]

In the spectra, the effect of stiffness changes was less pronounced, visible only as the expected slight increase in the progressive spacing of the partials. Hall and Askenfelt have shown that one effect of stiffness is a slight reduction of the magnitude of the higher components.[8]

The influence of string stiffness on hammer force is rather small in comparison with other parameters, which confirms the results obtained by Hall.[3] The simulated forces show variations of about $\pm 0.5\%$ of the maximum, as the string stiffness is varied by $\pm 50\%$, and the duration remains the same.

B. Hammer-string mass ratio

The influence of changing the hammer-string mass ratio was most clearly reflected in the interacting force between hammer and string. Figure 10(a)–(c) show hammer forces for the notes C2, C4 and C7, each note including three cases corresponding to different hammer-string mass ratios: Halved, nominal, and doubled, respectively (see Table I). It can be seen that a major effect of making the hammer heavier is to increase the contact duration, and vice versa. For the notes C4 and C7, the increase is roughly $\pm 30\%$ for a doubling and halving in hammer-string mass ratio, respectively. For the bass note (C2), the results are not symmetrical. The change in the contact duration for a halving in hammer-string mass ratio is similar to the two other notes (-20%), but with doubled hammer mass a clear case of multiple contacts develops and the total duration is extended considerably ($+60\%$).

It is interesting to note that a change in the hammer-string mass ratio does not influence the smoothness of the force waveform to any appreciable extent. This is in contrast to the cases where the dynamic level was changed (Fig. 4), or when exchanging hammers (Fig. 8), in which the force waveform peaked with increasing hammer velocity, and increasing stiffness, respectively. Here, the main effect is instead to increase the number of pulses returning from the agraffe as the hammer-string mass ratio increases, a heavier hammer requiring more accumulated impulses from the agraffe reflections in order to leave the string.

Naturally, the changes in hammer-string mass ratio are also visible in the string waveform, as well as in the force acting on the bridge. The bridge forces corresponding to the C4 examples in Fig. 10(b) are shown in Fig. 12(a). It can be seen that the amplitude of the bridge force increases with the hammer mass, accompanied by an increase of the width of the pulses due to the extended hammer-string contact. Interestingly, the repeated agraffe reflections, more pronounced in the case with the heavy hammer as mentioned, are clearly visible also in the bridge force waveform. This periodicity, which corresponds to the "missing partials" in the spectra due to striking position, are further discussed in the next section (see Sec. II C).

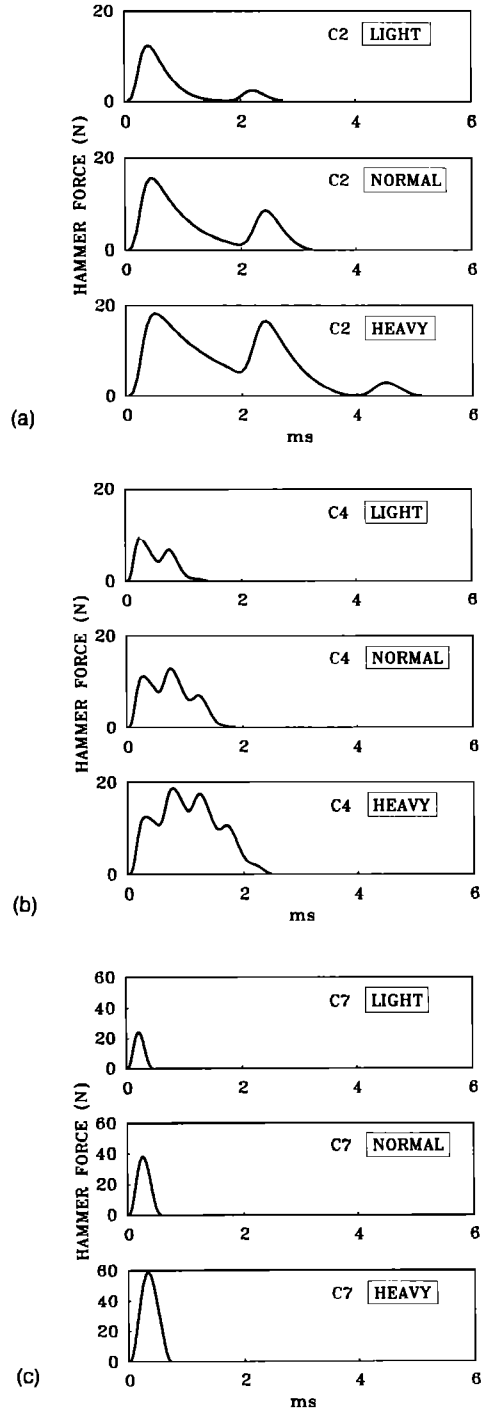

FIG. 10. Influence of hammer-string mass ratio. Simulated hammer forces for a (a) bass (C2), (b) mid (C4), and (c) treble note (C7), for three cases of hammer-string mass ratio; light (-50%), normal, and heavy ($+100\%$). Actual mass ratios M_H/M_S were (C2) 0.07, 0.14, and 0.28; (C4) 0.375, 0.75, and 1.5; (C7) 2.36, 4.71, and 9.42.

In the experiments reported above, variations of the hammer-string mass ratio were obtained through variations of the hammer mass only. The same values of the hammer-string mass ratio can, of course, be obtained through variations of the string mass, the hammer mass remaining constant. In that case, it becomes necessary to adjust the tension of the string in order to keep the fundamental frequency constant, but as a consequence the characteristic impedance of the string will be modified. It is

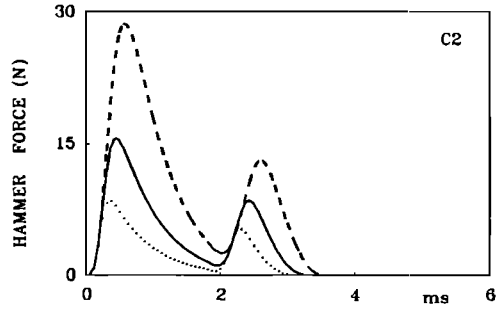

FIG. 11. Influence of string and hammer masses. Simulated hammer forces for a bass (C2) note, for a fixed normal hammer-string mass ratio M_H/M_S (0.14). The three curves correspond to the nominal case (full line), doubling (dashed line), and halving (dotted line) of hammer and string masses, respectively.

interesting to notice in this latter case that the duration of hammer-string contact doesn't depend significantly on the string mass. In the example shown in Fig. 11 for note C2, it can be seen that the contact time increases by only 5%, for a doubling of the string mass. By contrast, the magnitude of the force pulses are roughly proportional to the string masses, which is in accordance with the balance of forces at the striking point.

For the notes of the instrument where the pulses in the bridge force are clearly separated, i.e., in the low and medium range of the keyboard, the main differences in the spectra between the three cases with light, normal and heavy hammers, respectively, are found in the upper partials. An example is given for the bridge force of string C4 in Fig. 13(a), where the heavy-hammer spectrum has dropped 10 dB compared to the light-hammer case. This is a consequence of the broadening of the string pulses, which corresponds to a lower cutoff frequency. Also, a slightly weaker fundamental could be observed for the light-hammer case.

In the upper range of the keyboard, as illustrated by the C7 example, bridge forces obtained with different hammer-string mass ratios show an interesting detail [see Fig. 12(b)]. Here, the smoothest waveform is obtained with the nominal value of hammer-string mass ratio, and *not* with the highest hammer-string mass ratio like in the previous example for note C4. For the light hammer case, the pulses are narrow enough to just become separated, with a hint of zero displacement in between. In the heavy hammer case, the waveform becomes more peaked and triangular, and the first pulse is clearly higher than the following, both phenomena being the result of overlapping between pulses.

In the spectral domain, the C7 case with nominal hammer-string mass ratio (corresponding to a real instrument) gives the least amount of high-frequency energy. In particular, the difference compared to the light-hammer case is substantial with a clearly steeper spectral slope for the nominal case, resulting in a 10-dB level difference at 12 kHz [see Fig. 13(b)]. For the two lowest partials, the heavy-hammer case shows a steeper slope in spectral level than for the nominal case, like in Fig. 13(a), but for frequencies above 4 kHz, a "sawtooth" pattern with more

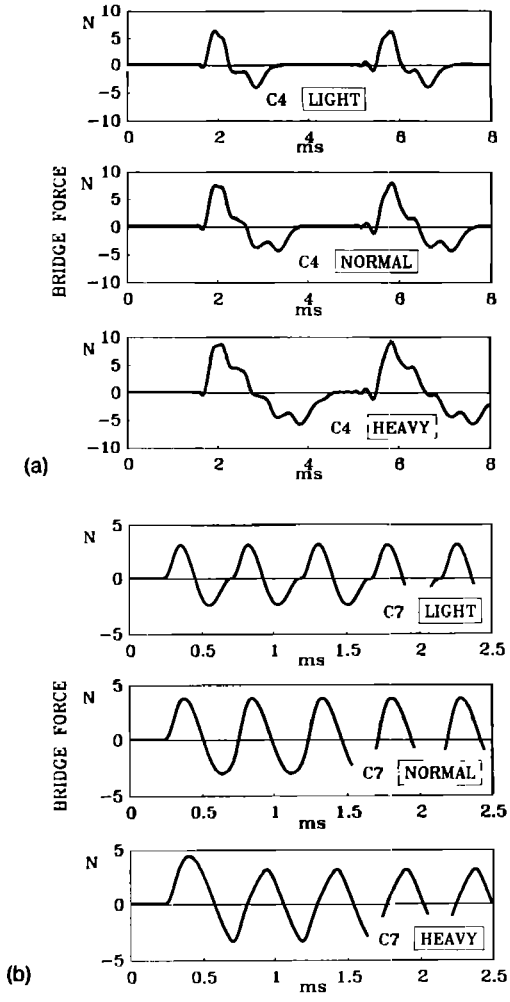

FIG. 12. Influence of the hammer-string mass ratio. Simulated forces at the bridge for three cases of hammer-string mass ratio; light, normal, and heavy. (a) Midrange, C4 [corresponding to Fig. 10(b)]; (b) treble, C7 [corresponding to Fig. 10(c)].

energy in the high-frequency range is observed. Intermediate values of hammer-string mass ratio have also been investigated, showing that the nominal value corresponds to the steepest slope with a smooth pattern.

It is an open question, whether the manufacturers are aware of the existence of this "least high-frequency ratio" for the hammer and string masses, and if this is exploited in the design. All three examples in Fig. 12(b) have been observed in measurements on real pianos, however, at different parts in the treble depending on manufacturer and instrument size.

C. Striking ratio

The influence of the relative hammer striking position (striking ratio) was also investigated. Figure 14(a) shows the changes in waveform and duration of the hammer force for note C4, as the striking ratio was varied between 0.04 (1/25) and 0.24 (1/4.2). The nominal value for the C4 simulations was 0.12 ($\approx 1/8$), which is representative for the striking ratios for this note in most pianos (between $1/9 \approx 0.11$ and $1/7 \approx 0.14$). As expected, it can be seen that the reflections returning from the agraffe become more and

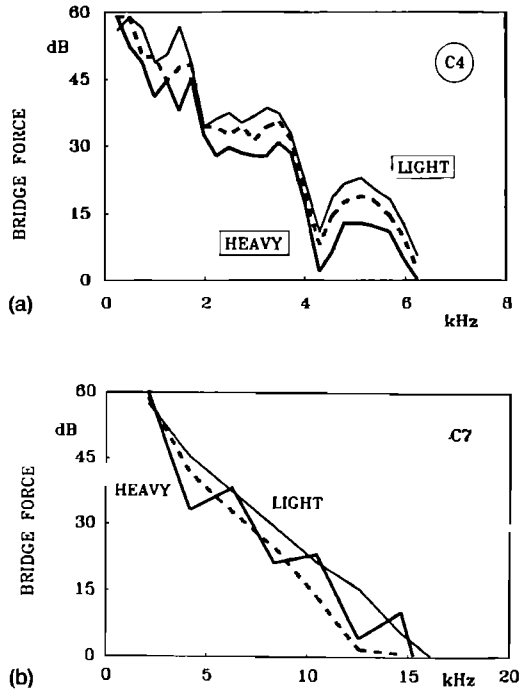

FIG. 13. Spectral envelopes corresponding to the initial 32 ms of the simulated bridge forces in Fig. 12, showing (a) note C4, and (b) note C7,with three hammer-string mass ratios; light (thin line), normal (dashed), and heavy (broad line). The actual mass ratios M_H/M_S are the same as in Fig. 10.

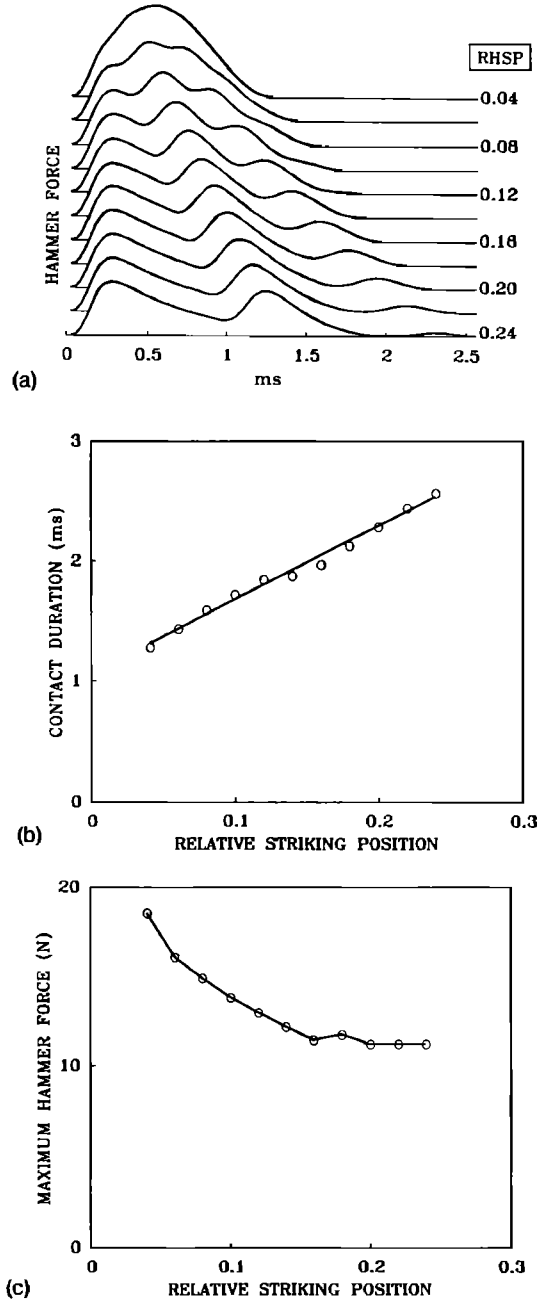

FIG. 14. Influence of relative hammer striking position α for note C4. (a) Simulated hammer forces for α between 0.04 and 0.24, (b) hammer-string contact duration versus α, (c) maximum hammer force versus α.

more separated and pronounced, as the striking ratio is increased. For a very short striking ratio (0.04) the force resembles a smooth hump, while for the nominal case and for longer striking ratios, two distinctive agraffe reflections can be observed in the force waveform. As the release of the hammer from the string is dependent on the accumulated effect of several agraffe reflections impinging on the hammer,[8] the contact duration increases as the striking ratio is increased. In the simulations, the relation between striking ratio and contact duration was found to be essentially linear [see Fig. 14(b)]. For the C4 note, the contact duration doubled for a sixfold increase in striking ratio (0.04 to 0.24).

The change in hammer-string interaction with increasing striking ratio, characterized by a progressive division of one broad force hump into several separated pulses, is illustrated in an alternative way in Fig. 14(c). This figure shows how the maximum value of the force pulse decreases as the striking ratio is increased, meaning that, for small relative hammer striking positions, the accumulation of agraffe reflections doesn't allow the force to decay in between.

The influence of the striking ratio on the force waveform at the bridge, and on the corresponding spectra, was studied for a bass note (C2), by halving and doubling the nominal striking ratio (see Fig. 15). The well-defined pattern for a short striking ratio, with pulses at the fundamental period spacing, is successively more and more "disturbed" by pulses in between, as the striking ratio is increased. These interfering pulses correspond to the increasingly delayed first and second agraffe reflections (indicated by A1 and A2).

In the frequency domain, the effect of increasing the striking ratio is seen mainly in the periodical pattern punctuating the spectral envelope with weak modes corresponding to the inverse of the striking ratio (see Fig. 16). The repetition rate of the agraffe reflections, interfoliating the fundamental pulses, correspond to these "missing modes"-frequencies, but they are not strong enough to fill up the gaps in the spectra, when they are "given to" the string at the end of the string contact.[14,15] The overall spectral slope does not change as the striking ratio is varied.

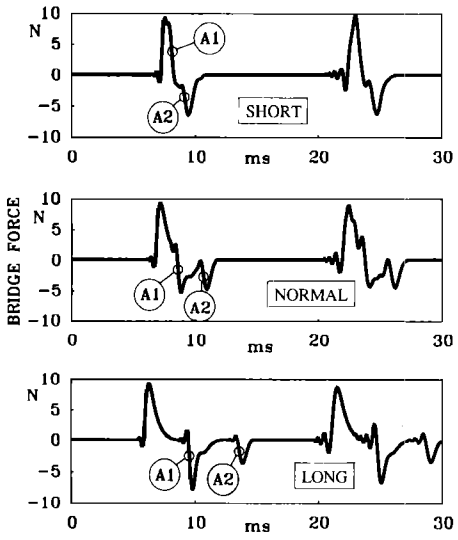

FIG. 15. Influence of striking position for note C2. Simulated force at the bridge for three cases of increasing relative hammer striking position; short (−50%), normal, and long (+100%). The value for the relative striking position was =0.06, 0.12, and 0.24, respectively. The first and second reflections from the agraffe are indicated by A1 and A2, respectively.

III. CONCLUSIONS

The evaluation of our numerical model has shown that it is capable of reproducing the characteristic features of real piano strings in both the time and frequency domain. The influence of the control parameters for the excitation of the struck string (such as initial hammer velocity and felt compression properties), discussed by several authors,[3,7,16] has been confirmed. In addition, informal listening tests have shown that the synthesized tones sound very similar to the vibrations of real piano strings, as recorded by appropriate string transducers. The influence of the frequency-dependent damping, which is relatively hard to see in the waveforms, is clearly audible.

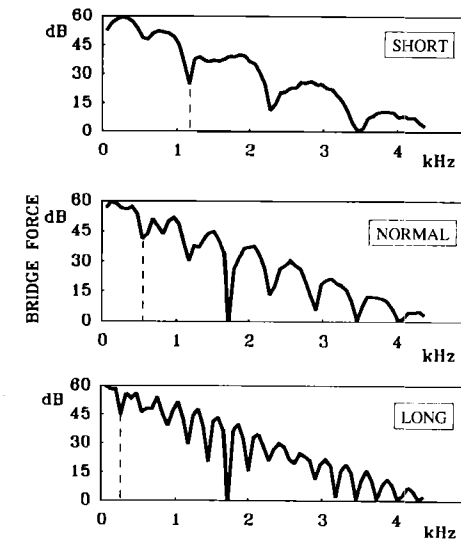

FIG. 16. Spectra of the simulated bridge forces in Fig. 15 for note C2 with three relative hammer striking positions; short, $\alpha=0.06$ (1/16.7), normal, $\alpha=0.12$ (1/8.3), and long, $\alpha=0.24$ (1/4.2). The dashed vertical lines indicate the first minima due to the relative striking position.

The flexibility of the simulation program makes it possible to use the model as a efficient tool for exploring a wide range of physical parameters, such as string stiffness, hammer-string mass ratio, and relative hammer striking position. Such a systematic exploration of the piano design, guided by a perceptual evaluation, is probably one of the major features of sound synthesis by physical modeling.

Our numerical model of the piano string is still far from complete. Among other things, the boundary conditions are modeled in a rather crude way. Work in progress include an attempt to terminate the last segment of the string by a realistic load, obtained from admittance measurements at the bridge of a real piano (at the point where the actual string crosses). Pilot experiments have already been conducted with simulations of a triplet of slightly detuned C6 strings coupled by the bridge, using existing measurements of the soundboard admittance.[17] This approach has given significant improvements in the realism of the synthesis. By including a modeling of the two directions of string polarization, one in parallel and one perpendicular to the soundboard, we expect to obtain a more realistic decay process, due to the energy exchange between the two families of modes.[18] For this purpose, some preliminary measurements of the admittance matrix at the bridge will be necessary.

Presently, it must be admitted that the simulated tones don't mimic real piano tones convincingly when listening, a slightly disappointing fact. The essential missing feature in the synthesis is in the attack component, which for a real piano tone includes a strong "thump." This component is due to the shocklike excitation of the whole instrument at the impact of the hammer on the string. A large part of the thump originates from the soundboard, which is set in motion almost immediately at the hammer impact by a longitudinally transmitted pulse train reflecting between bridge and hammer. This longitudinal motion precedes the first transversal string pulse 1–2 ms (midrange).[11] A good illustration of this effect can be obtained by isolating the string transmitted thump from the "sounding" part of the tone by damping the transversal string motion (with the hand).

Other transient components are excited by the inertial force of the accelerating hammer, as well as the touch force on the key, which both are transmitted to the iron plate and soundboard via the key bed and rim. An example of the attack components, as registered at the bridge, is shown in Fig. 17, for a case where the strings have been removed and the hammer strikes a dummy mass. This was done in order to avoid a masking of the attack components by the much stronger string vibrations. Interestingly, it appears that the particular history of the attack components are affected by the pianist's type of touch.

By adding a recording of the attack components (with damped strings) to the computer simulations, significant improvements in the realism of the synthesis were obtained. This has encouraged us to continue the modeling of

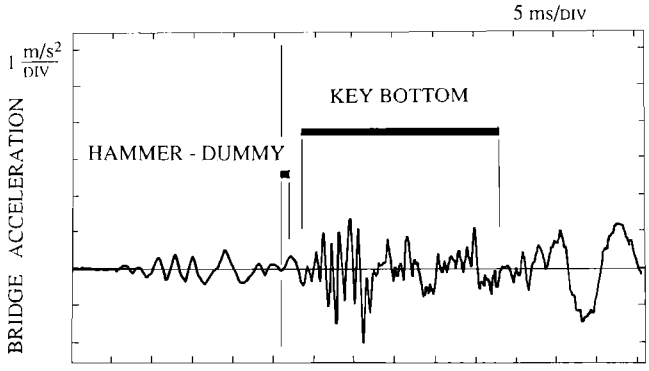

FIG. 17. Registration of the acceleration at the bridge with the strings removed and the hammer striking a dummy mass (C4, *forte, staccato*-touch). The signals representing hammer-dummy contact, and key bottom position, are included for reference (horizontal bars). The bridge motion starts with a percussive component about 20 ms before hammer-dummy contact, followed by a "wave package" at about 1000 Hz (due to a resonance in the key). Later, the motion is dominated by a mixture of resonances in the key bed at 100 and 250 Hz, approximately. The vibration level of these pre- and postcursors is of the same order as the bridge variations due to string motion at *pp* level.

the longitudinal vibrations of the string, once the soundboard admittance at the bridge termination have been satisfactorily implemented.

ACKNOWLEDGMENTS

Part of this work was conducted during Fall 1990, when the first author was a guest researcher at the Department of Speech Communication and Music Acoustics, Royal Institute of Technology (KTH), Stockholm, with financial support from Centre National de la Recherche Scientifique (CNRS). The project was further supported by the Swedish Natural Science Research Council (NFR), the Swedish Council for Research in the Humanities and Social Sciences (HSFR), the Bank of Sweden Tercentenary Foundation, and the Wenner-Gren Center Foundation. The authors wish to thank Xavier Boutillon and an anonymous reviewer for helpful comments on a previous version of this paper.

[1] A. Chaigne and A. Askenfelt, "Numerical simulation of piano strings. I: A physical model for a struck string using finite difference methods," J. Acoust. Soc. Am. **95**, 1112–1118 (1994).
[2] H. Suzuki and I. Nakamura, "Acoustics of pianos," Appl. Acoust. **30**, 147–205 (1990).
[3] D. Hall, "Piano string excitation. VI: Nonlinear modeling," J. Acoust. Soc. Am. **92**, 95–105 (1992).
[4] A. Askenfelt and E. Jansson, "From touch to string vibrations—The initial course of the piano tone," Speech Transmission Lab. Quarterly Progress and Status Report, Dept. of Speech Communication and Music Acoustics, Royal Institute of Technology, Stockholm, STL-QPSR **1**, 31–109 (1988).
[5] A. Askenfelt and E. V. Jansson, "From touch to string vibrations. III: "String motion and spectra," J. Acoust. Soc. Am. **93**, 2181–2196 (1993).
[6] J. Nakamura, "The vibration of a struck string (Acoustical research on the piano. Part 1)," J. Acoust. Soc. Jpn. (E) **13**(5), 311–321 (1992).
[7] X. Boutillon, "Model for piano hammers: Experimental determination and digital simulation," J. Acoust. Soc. Am. **83**, 746–754 (1988).
[8] D. Hall and A. Askenfelt, "Piano string excitation. V. Spectra for real hammers and strings," J. Acoust. Soc. Am. **83**, 1627–1638 (1988).
[9] D. Hall, "Piano string excitation in the case of a small hammer mass," J. Acoust. Soc. Am. **79**, 141–147 (1986).
[10] T. Yanagisawa and K. Nakamura, "Dynamic compression characteristics of piano felt," J. Acoust. Soc. Jpn. **40**, 725–729 (1984) (in Japanese).
[11] A. Askenfelt and E. V. Jansson, "From touch to string vibrations. II: "The motion of the key and hammer," J. Acoust. Soc. Am. **90**, 2383–2393 (1991).
[12] D. Hall, "Piano string excitation. II: General solution for a hard narrow hammer," J. Acoust. Soc. Am. **81**, 535–546 (1987).
[13] M. Podlesak and A. Lee, "Dispersion of waves in piano strings," J. Acoust. Soc. Am. **83**, 305–317 (1988).
[14] A. H. Benade, *Fundamentals of Musical Acoustics* (Oxford, U.P., New York, 1976), Chap. 17.
[15] D. Hall and P. Clark, "Piano string excitation. IV: The question of missing modes," J. Acoust. Soc. Am. **82**, 1913–1918 (1987).
[16] H. Suzuki, "Model analysis of a hammer-string interaction," J. Acoust. Soc. Am. **82**, 1145–1151 (1987).
[17] K. Wogram, "Acoustical research on pianos: Vibrational characteristics of the soundboard," Das Musikinstrument **24**, 694–702, 776–782, 872–880 (1980).
[18] G. Weinreich, "Coupled piano strings," J. Acoust. Soc. Am. **62**, 1474–1484 (1977).